Edge Intelligence Empowered UAVs for Automated Wind Farm Monitoring in Smart Grids

Hwei-Ming Chung*, Sabita Maharjan*†, Yan Zhang*†, Frank Eliassen*, and Tingting Yuan‡
* Department of Informatics, University of Oslo, 0373 Oslo, Norway
† Simula Metropolitan Center for Digital Engineering, 0167 Oslo, Norway
‡ Institute of Computer Science, Georg-August-University of Göttingen, 37073 Göttingen, Germany
Emails: *hweiminc@ifi.uio.no, sabita@ifi.uio.no, yanzhang@ieee.org, frank@ifi.uio.no ‡tingt.yuan@hotmail.com

GLOBECOM 2020 - 2020 IEEE Global Communications Conference | 978-1-7281-8298-8/20/$31.00 ©2020 IEEE | DOI: 10.1109/GLOBECOM42002.2020.9322269

***Abstract*—With the exploitation of wind power, more turbines will be deployed at remote areas possibly with harsh working conditions (e.g., offshore wind farm). The adverse working environment may lead to massive operating and maintenance costs of turbines. Deploying unmanned aerial vehicles (UAVs) for turbine inspection is considered as a viable alternative to manual inspections. An important objective of automated UAV inspection is to minimize the flight time of the UAVs to inspect all the turbines. A first contribution of this paper is thus formulating an optimization problem to compute the optimal routes for turbine inspection satisfying the above goal. On the other hand, the limited computational capability on UAVs can be used to increase the power generation of wind turbine. Power generation from the turbines can be optimized by controlling the yaw angle of the turbines. Forecasting wind conditions such as wind speed and wind direction is crucial for solving both optimization problems. Therefore, UAVs can utilize their limited computational capability to perform wind forecasting. In this way, UAVs form edge intelligence in offshore wind farm. With the forecasted wind conditions, we design two algorithms to solve the formulated problems, and then evaluate the proposed methods with real-world data. The results reveal that the proposed methods offer an improvement of 44% of the power generation from the turbine compared to hour-ahead forecasting and 25% reduction of the flight time of the UAVs compared to the chosen baseline method.**

***Index terms*– unmanned aerial vehicle (UAV), edge intelligence, wind forecast, turbine control, routing problem.**

I. Introduction

Wind power is a clean alternative to address climate change and to reduce our dependence on fossil fuel power. The total capacity of the installed wind power in Europe is expected to reach 350 GW by 2030, which can support 24% of the European electricity consumption [1]. Also, grid operators can operate power grids with flexibility by utilizing wind power so as to form a smart grid. This goal requires more wind turbines to be installed. However, turbines may suffer from failure of components, such as blades, gearbox, and yaw system [2], which can affect the efficiency of the turbine and can also lead to compete operation failure. For example, a blade failure can result in a downtime of more than seven days [3].

Currently, the inspection of wind turbines is done manually by qualified service personnel. This procedure can take from several days to several weeks, requiring intensive and costly efforts. Moreover, the workers are exposed to variable wind conditions and harsh environments in offshore wind farms. To reduce the utilization of manpower, unmanned aerial vehicles (UAVs) can play a crucial role in automating the inspection of wind turbines. For instance, cracks on the surface of turbine blades can be detected with the help of images taken by UAVs [4], [5]. Additionally, UAVs can be embedded with various advanced sensors such as Lidar sensors [6], thermal-wave radar [7], and millimeter wave imaging [8] to detect the failure of wind turbines. With advanced sensors, automated inspection with UAVs has also been studied in [9], [10]. In [9], UAVs with thermal-wave radar were utilized to monitor the condition of solar panels. The inspection of power lines using UAVs was proposed in [10] so that workers do not need to climb the transmission line tower. In the context of the smart grid, automatic meter reading is another application of UAVs in power systems [11]. UAVs combined with fault indicators was proposed in [12] to deliver signal from the fault indicators to the operator in case of damage on the distribution line.

UAVs have also obtained some computational capabilities and therefore UAVs can also be applied to facilitate computing service at remote sites. That is, computation can be moved closer to the edge of the network (i.e., UAVs) such that data can be processed physically close to where the data is generated. In [13], optimal UAV-routes were computed for UAV assisted inspection of wind turbines under different wind conditions. That is, UAVs can observe current wind condition and then computational resources of the UAVs can be utilized to calculate the optimal routing paths for inspection. More recently, combining machine learning algorithms with the computational resources of the UAVs has become a promising approach towards managing more complicated tasks, thus giving rise to the term "edge intelligence". UAVs were utilized to schedule the transmission of the signal for users to prevent from jamming by applying deep reinforcement learning [14]. [15] is a recent work in this context where the authors proposed a framework where UAVs utilized long short term memory (LSTM) to predict the upcoming tasks and then to find the optimal position to serve mobile users.

In previous works, UAVs were mainly regarded as relays in [14], [15] and as inspection tools in [9]–[12]. However, sensors embedded in UAVs can be utilized for remote sensing [16]. That is, Lidar sensors [6] can be applied to collect the meteorological measurements in the wind farm. UAVs acting as computing units can provide information (e.g., wind speed and wind direction) to wind turbines thus playing a

978-1-7281-8298-8/20/$31.00 ©2020 IEEE

significant role in controlling the operation of wind turbines. Specifically, it is expected that wind farms become larger and larger in the near future while the capacity of turbines is also increasing. Small variation of wind conditions in large wind farms considerably affect the power generation of wind turbines with high capacity. In this case, UAVs can obtain high-resolution meteorological measurements from remote sensing and then forecast weather conditions to turbines, so that the wind turbines can operate at their optimal conditions to generate maximum power. Moreover, the forecasting information supplies valuable information for the decision-making of the routes for turbine inspection. For computation necessary for forecasting however, it is required to consider the limited computational capabilities and storage space on UAVs.

In this paper, we utilize UAVs to form the edge intelligence units in an offshore wind farm. That is, we utilize UAVs as remote sensing units to collect the meteorological measurements in offshore wind farms. With the measurements, UAVs can inspect the turbines and can also control the operation of wind turbines by adjusting the yaw angle. In this regard, we formulate a control optimization problem to maximize power generation from turbines and an optimization problem to find the optimal routing path for automated turbine inspection by UAVs. To solve the problems, UAVs forecast the wind speed and wind direction based on the measurements collected by sensors embedded in the UAV. Moreover, we take into account the hardware limitation of the UAVs for forecasting wind speed and wind direction based on machine learning method. Then, we design two algorithms to solve the formulated problems by making use of the forecasting results as inputs. To this end, our main contributions in this paper are threefold:

- We present a new framework for utilizing UAVs as edge intelligence units to facilitate automated wind farm monitoring. That is, we formulate an optimization problem for maximizing the power generation of turbines and a UAV-route optimization problem for turbine inspection.
- We design heuristic algorithms to derive the optimal condition for operating wind turbines and the optimal path for the inspection with forecasted wind as input. The results reveal that 25% reduction on the flight time compared to the baseline method and 44% increase in power generation compared to hour-ahead forecasting.
- UAVs have some computational capabilities and storage space. Therefore, we take the limited computational capabilities and storage space on UAVs into account when forecasting the wind speed and wind direction by LSTM.

II. System Model

A. Wind and Wind Turbine Model

We denote the wind velocity by $\mathbf{w} = [w^x, w^y]$, where w^x and w^y represent the projection of the wind velocity on the x-axis and the y-axis, respectively. The wind speed, denoted by w_s, is calculated from $w_s = ||\mathbf{w}||_2$. Let θ_w^{pol} be the wind direction in the polar coordinate system defined as $\theta_w^{pol} = \arctan \frac{w^y}{w^x}$. The representation of wind direction in the meteorological measurements is different from θ_w^{pol}. In this case, we define the wind direction in the meteorological measurements as θ_w^{met}. Phases 0, $\frac{\pi}{2}$, π, and $\frac{3\pi}{2}$ are used to represent the north, the east, the south, and the west wind in the meteorological measurements, respectively. With this notion, the phase is represented in a clockwise direction. In the polar coordinate system however, the phase is represented in a counterclockwise direction. Therefore, θ_w^{pol} and θ_w^{met} are related as $\theta_w^{pol} = \frac{3\pi}{2} - \theta_w^{met}$.

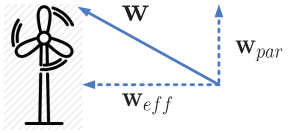

Fig. 1. The relation between a wind turbine and the wind velocity.

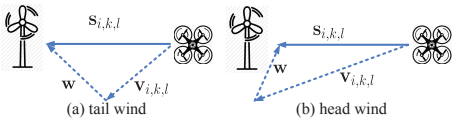

Fig. 2. The relation between a UAV, a wind turbine, and the wind velocity.

The coordinates of the k-th turbine in the wind farm are $\mathbf{q}_k = [x_k, y_k]$. Then, according to [17] and [18], the power generation of the k-th turbine can be represented as

$$p_k = \frac{1}{2}\rho A w_s^3 C_p(\lambda, \beta), \tag{1}$$

where A is the blade sweep area and ρ is the air density. Function C_p represents the power coefficient of the turbine based on λ and β. Quantities λ and β are the pitch angle of wind turbine and the tip speed ratio, respectively. However, for a wind turbine, the power generation is only affected by the wind velocity that is perpendicular to the turbine. Therefore, w_s in (1) should be replaced. Wind velocity can be separated into two components, $\mathbf{w}_{eff}$ and $\mathbf{w}_{par}$, which respectively represent the wind direction perpendicular and parallel to the turbines. In this case, the power generation of turbines is only affected by $\mathbf{w}_{eff}$. We then replace w_s in (1) with $||\mathbf{w}_{eff}||_2$. The relation between a turbine and wind velocity is shown in Fig. 1.

B. UAV Model

We consider a total of N UAVs in an offshore wind farm to inspect the condition of the turbines. Each UAV $i = 1, ...N$, is placed at $\mathbf{q}_i = [x_i, y_i]$. The set of turbines for UAV i to inspect is denoted by $\mathcal{N}_i$, and $|\mathcal{N}_i|$ represents the cardinality of set $\mathcal{N}_i$.

When inspecting the turbines, wind speed and wind direction must be considered for deriving the optimal UAV-route for turbine inspection. Thus, UAV i may face two wind conditions, namely tail wind and head wind, as shown in Fig. 2. We define $\mathbf{s}_{i,k,l}$ and $\mathbf{v}_{i,k,l}$ as the resultant velocity and the UAV velocity of UAV i flying from turbine k to turbine l, respectively. Vector $\mathbf{v}_{i,k,l}$ is the initial velocity of the UAV, and the resultant velocity is defined by the velocity influenced by the wind velocity. The angle between $\mathbf{s}_{i,k,l}$ and $\mathbf{v}_{i,k,l}$ is denoted by $\theta_{i,k,l}^{s,v}$ and $\theta_{i,k,l}^{s,w}$ is defined as the angle between $\mathbf{s}_{i,k,l}$ and $\mathbf{w}$. The relation between $\mathbf{v}_{i,k,l}$, $\mathbf{s}_{i,k,l}$, and $\mathbf{w}$ is expressed as

$$\mathbf{v}_{i,k,l} + \mathbf{w} = \mathbf{s}_{i,k,l}. \quad (2)$$

We then define the airspeed and the groundspeed as $||\mathbf{v}_{i,k,l}||_2$ and $||\mathbf{s}_{i,k,l}||_2$, respectively. The flying speed limit is denoted by u_i^{max}.

The flight time for UAV i traveling from turbine k to turbine l can be calculated as

$$t_{i,k,l} = \frac{||\mathbf{q}_l - \mathbf{q}_k||_2}{||\mathbf{s}_{i,k,l}||_2}. \quad (3)$$

The maximum flight time of UAV i is denoted by t_i^{max}, which represents the upper limit on the total flight time during inspection. The distance between UAV i and turbine k is $d_{i,k}$.

The flying range of UAV i can be expressed as

$$B_i(\rho_i) = \{x, y \in \mathbb{R} : ||\mathbf{r}||_2 \leq \rho_i\}, \quad (4)$$

where $\mathbf{r} = [x - x_i, y - y_i]$. The quantity ρ_i is the actual flying distance of UAV i, which is defined by the operator. As in (4), we regard the flying range of the UAV as a circle, with the location of UAV i, $[x_i, y_i]$ as the center of the circle.

III. Problem Formulation

In this section, we formulate a control optimization problem to obtain the maximum power generation from the wind turbines. Then, we formulate a routing optimization problem to find the best UAV path for the inspection. Wind is a very important factor in determining the flying range and flying speed of UAVs. We therefore also incorporate the influence of the wind speed and the wind direction into the routing optimization problem.

A. Power Generation Maximization with Yaw Control

Let θ_k^{yaw} be the yaw angle that can be adjusted to generate the maximum power generation of the k-th turbine Let $\theta_k^{w,yaw}$ denote the angle between $\mathbf{w}$ and θ_k^{yaw}. With these notations, an optimization problem for maximizing the power generation of the turbine can be formulated as

$$\max_{\theta_k^{yaw}} \quad p_k \quad (5a)$$

$$\text{subject to} \quad 0 \leq \theta_k^{yaw} \leq 2\pi, \quad (5b)$$

$$0 \leq p_k \leq p_k^{max}, \quad (5c)$$

$$||\mathbf{w}_{eff}||_2 = w_s \cos(\theta_k^{w,yaw}). \quad (5d)$$

The yaw angle of the turbine is limited between 0 and 2π as indicated in (5b). Constraint (5c) implies that the power generation of turbines cannot exceed the rated power, p_k^{max}. The power generation is affected by the wind direction perpendicular to the turbine, $||\mathbf{w}_{eff}||_2$, which is given by (5d).

B. Routing Optimization of UAVs

Let M_i denote the number of required routes for UAV i to inspect the turbines. We introduce matrix $\mathbf{U}_i^m = [U_{i,k,l}^m]_{|\mathcal{N}_i|\times|\mathcal{N}_i|}$ to denote the m-th route for UAV i. If UAV i chooses to fly from turbine k to turbine l, $U_{i,k,l}^m$ is 1; otherwise, $U_{i,k,l}^m$ is 0. The optimal routing problem can then be formulated as

$$\min_{\substack{M_i, \mathbf{U}_i^m, \mathbf{v}_{i,k,l}, \\ \mathbf{s}_{i,k,l}, \theta_{i,k,l}^{s,v}}} \quad t^{ins} = \sum_i \sum_{m=1}^{M_i} \sum_{k\in\mathcal{N}_i} \sum_{l\in\mathcal{N}_i\setminus\{k\}} t_{i,k,l} U_{i,k,l}^m \quad (6a)$$

$$\text{subject to} \quad \sum_{k\in\mathcal{N}_i} U_{i,s,k}^m = \sum_{k\in\mathcal{N}_i} U_{i,k,s}^m = 1, \quad \forall m, i \quad (6b)$$

$$\sum_{l\in\mathcal{N}_i\setminus\{l\}} U_{i,l,k}^m = \sum_{l\in\mathcal{N}_i\setminus\{k\}} U_{i,k,l}^m = 1, \forall m, i \quad (6c)$$

$$U_{i,k,l}^m \in \{0,1\}, \qquad \forall k, l \in \mathcal{N}_i, \forall i \quad (6d)$$

$$\sum_{k\in Q}\sum_{l\in Q} U_{i,k,l}^m \leq |Q|-1, \forall Q \subsetneq \mathcal{N}_i, m, \forall i \quad (6e)$$

$$1 \leq M \leq |\mathcal{N}_i| - 1, \qquad \forall i \quad (6f)$$

$$\sum_{k,l\in\mathcal{N}_i} t_{i,k,l} U_{i,k,l}^m \leq t_i^{max}, \qquad \forall m, i \quad (6g)$$

$$||\mathbf{v}_{i,k,l}||_2 \leq u_i^{max}, \qquad \forall k, l \in \mathcal{N}_i, \forall i \quad (6h)$$

$$||\mathbf{s}_{i,k,l}||_2 \leq u_i^{max}, \qquad \forall k, l \in \mathcal{N}_i, \forall i \quad (6i)$$

$$\mathbf{v}_{i,k,l} + \mathbf{w} = \mathbf{s}_{i,k,l}, \qquad \forall k, l \in \mathcal{N}_i, \forall i \quad (6j)$$

In (6), the objective is to minimize the flight time and the number of routes for all UAVs in the wind farm to inspect all the turbines. The location of the UAV is regarded as a starting point, $s = \mathbf{q}_i$, as indicated in (6b). Then, only one route can be obtained between turbines as stated in (6c). The path of routing during inspection, $U_{i,k,l}^m$, is restricted to a binary parameter in (6d). Constraint (6e) ensures that a closed path does not exist in the subset Q of $\mathcal{N}_i$. The number of routes for the inspection should be less than the number of turbines in $\mathcal{N}_i$ as stated in (6f). For every route, the total flight time cannot exceed t_i^{max} according to (6g). The airspeed and groundspeed should be bounded by u_i^{max} as mentioned in (6h) and (6i), respectively. The relationship between the wind velocity, the UAV velocity, and the resultant velocity mentioned in (2) is given by (6j).

IV. Algorithm Design

To design our algorithms, we require the future wind condition (i.e., wind speed and wind direction) as input. UAVs acting as remote sensing units in wind farms can obtain meteorological measurements with high resolution. In this case, these measurements can be applied to perform wind forecasting. The UAVs have limited computational capabilities and storage space, and therefore we need to consider the hardware limitation when performing wind forecasting.

A. Wind Forecasting with Low-precision LSTM

We introduce LSTM to UAVs to forecast the wind speed and the wind direction, and the structure of LSTM can be described as

$$f_i = \sigma_g(\mathbf{W}_f \mathbf{x}_t + \mathbf{U}_f \mathbf{h}_{t-1} + \mathbf{b}_f), \quad (7a)$$

$$i_i = \sigma_g(\mathbf{W}_i \mathbf{x}_t + \mathbf{U}_i \mathbf{h}_{t-1} + \mathbf{b}_i), \quad (7b)$$

$$o_t = \sigma_g(\mathbf{W}_o \mathbf{x}_t + \mathbf{U}_o \mathbf{h}_{t-1} + \mathbf{b}_o), \quad (7c)$$

$$c_t = f_t \circ \mathbf{c}_{t-1} + i_t \circ \sigma_c(\mathbf{W}_c \mathbf{x}_t + \mathbf{U}_c \mathbf{h}_{t-1} + \mathbf{b}_c), \quad (7d)$$

$$h_t = o_t \circ \sigma_h(\mathbf{c}_t), \quad (7e)$$

where $\circ$ denotes the Hadamard product. The input data is denoted by $\mathbf{x}_t$. In (7), f_i, i_i, o_t, c_t, and h_t are the forget gate, the input gate, the output gate, the cell state, and the hidden state, respectively. Then, $\mathbf{b}_f$, $\mathbf{b}_i$, $\mathbf{b}_o$, and $\mathbf{b}_c$ are the

bias vectors. To address the limitation of the hardware, we introduce the quantization to LSTM. We use ω_w to denote the number of bits of fixed-point integer to represent all elements in $\mathbf{W}_f$, $\mathbf{W}_i$, $\mathbf{W}_o$, $\mathbf{W}_c$, $\mathbf{U}_f$, $\mathbf{U}_i$, $\mathbf{U}_o$, and $\mathbf{U}_c$. The quantization model is represented as

$$Q_{\omega_w}(\mathbf{W}) = clip\left(\frac{\mathbf{W}}{\gamma \text{median}(|\mathbf{W}|)}, -0.5, 0.5\right) + 0.5, \quad (8)$$

where a natural choice of γ would be 2.5 [19], and the clip function is defined as

$$clip\,(\mathbf{W}) = \frac{1}{2^{\omega_w} - 1} \lfloor (2^{\omega_w} - 1)\mathbf{W} + 0.5 \rfloor, \quad (9)$$

where $\lfloor * \rfloor$ is the round function. In the final layer, we introduce a fully-connected layer to obtain the forecasted value, $\hat{y}_t$, as

$$\hat{\mathbf{y}}_t = \mathbf{W}_y h_t + \mathbf{b}_y. \quad (10)$$

In (10), $\mathbf{W}_y$ is quantized with ω_f bits and $\mathbf{b}_y$ is the corresponding bias vector.

With the quantized LSTM framework, we can further reduce the computational complexity for wind forecasting. According to [20], the weight matrix becomes sparse with quantization. Therefore, we further utilize the sparse matrix multiplication to the proposed framework.

B. Algorithms for Maximizing Power Generation

With the forecasted wind conditions, we can now solve problem (5). Before calculating power generation, UAVs calculate the power coefficient for the turbines (the optimal working condition for the turbines). Then, we obtain the power generation of the turbine by (1). We change the yaw angle to θ_w^{pol} when p_k is lower than the rated power. Adjusting the yaw angle is stopped when the power generation reaches the rated power. The details are provided in Algorithm 1. Then, the computational complexity of Algorithm 1 is $\mathcal{O}(|\mathcal{N}_i|)$, where it is only related to the number of turbines for UAV i to inspect.

Algorithm 1: Search the Optimal Yaw Angle

Input: $\hat{\mathbf{y}}_t$, ρ, A, θ_w^{pol}
Output: θ_k^{yaw}

Obtain $C_p(\lambda, \beta)$ by using the method in [17]
Compute the power generation with (1)
$\theta_k^{yaw} = \begin{cases} \theta_k^{yaw} = \theta_w^{pol}, & \text{if } p_k \le p_k^{max}, \\ \theta_k^{yaw} = \theta_k^{yaw}, & \text{if } p_k > p_k^{max}. \end{cases}$

C. Algorithms for Finding Optimal Routing Path

With the forecasted wind speed and wind direction, we can now obtain the solution of (6). The solving procedure is presented in Algorithm 2. At the beginning, the UAV calculates the flying range based on forecasted wind conditions, denoted by $B_i^{\hat{\mathbf{y}}_t}$. The center of $B_i^{\hat{\mathbf{y}}_t}$, $[\hat{x_r}, \hat{y_r}]$, is defined as

$$\hat{x_r} = x_i + w^x t_i^{max}, \quad \hat{y_r} = y_i + w^y t_i^{max}. \quad (11)$$

The new flying range of the UAV is the intersection of $B_i^{\hat{\mathbf{y}}_t}$ and B_i denoted by

$$Z_i = B_i^{\hat{\mathbf{y}}_t} \bigcap B_i. \quad (12)$$

Algorithm 2: Obtain the optimal routing path

Input: $\mathcal{N}_i$, $[x_i, y_i]$, B_i, $\hat{\mathbf{y}}_t$
Output: $U_{i,k,l}^m$

Set $\hat{\mathcal{N}}_i = \mathcal{N}_i$; $s = [x_i, y_i]$;
Calculate the flying range based on $\hat{\mathbf{y}}_t$
Perform the intersection of $B_i^{\hat{\mathbf{y}}_t}$ and B_i to get Z_i
Put the turbines out of new flying range to o_i
Sort o_i of all UAVs based on $|o_i|$ in a decreasing order with the index as $e_1, e_2, \ldots, e_N$
for $i = 1$ **to** N **do**
  while $o_{e_i} > 0$ **do**
    Take turbine k from o_{e_i}
    Assign turbine k to UAV j according to (13)
    $\mathcal{N}_i = \mathcal{N}_i \setminus \{k\}$; $o_{e_i} = o_{e_i} \setminus \{k\}$; $\hat{\mathcal{N}}_j = \hat{\mathcal{N}}_j \cup \{k\}$
Calculate $t_{i,k,l}$ with $k, l \in \hat{\mathcal{N}}_j$ by (3) and (14)
Use Branch-and-Cut algorithm to find the optimal path without considering (6g)
Separate route based on t_i^{max} to get $U_{i,k,l}^m$ for UAV i

With the new flying range, some turbines in $\mathcal{N}_i$ may beyond the range Z_i. The set of turbines outside Z_i is denoted by o_i. Then, we sort $|o_i|$ of all UAVs in decreasing order. We assign turbine k in o_i to UAV j based on

$$j = \left\{ \underset{j}{\text{argmin}}\, d_{j,k} | [x_k, y_k] \in Z_j \right\}. \quad (13)$$

The reassigned set of turbine to UAV i is denoted by $\hat{\mathcal{N}}_i$. Then, we use (3) to calculate $t_{i,k,l}$. Vector $\mathbf{s}_{i,k,l}$ is obtained from

$$\mathbf{s}_{i,k,l} = \begin{cases} [u_i^{max}\cos(\theta_s), u_i^{max}\sin(\theta_s)], & 0 \le \theta_{i,k,l}^{s,w} \le \frac{\pi}{2}, \\ [u_i^{s}\cos(\theta_s), u_i^{s}\sin(\theta_s)], & \frac{\pi}{2} < \theta_{i,k,l}^{s,w} \le \pi, \end{cases} \quad (14)$$

where θ_s is given by $\arctan((y_l - y_k)/(x_l - x_k))$. In (14), u_i^s can be calculated using $u_i^s = u_i^{max}\cos(\theta_{i,k,l}^{s,v}) - w_s\cos(\pi - \theta_{i,k,l}^{s,w})$, where $\theta_{i,k,l}^{s,v} = \arcsin(w_s \sin(\pi - \theta_{i,k,l}^{s,w})/u_i^{max})$. Then, we can use the relation in (2) to calculate $\mathbf{v}_{i,k,l}$. Finally, line 12 in Algorithm 2 (Algorithm 2 in [21]) was applied to find the optimal routing path without considering flight time constraint, (6g). Then, we separate the optimal path by considering t_i^{max} at line 13 in Algorithm 2 (Algorithm 3 in [21]). The computational complexity of Algorithm 2 is $\mathcal{O}\left(N\log(N) + N^2|o_i| + |\hat{\mathcal{N}}_i|^2 2^{|\hat{\mathcal{N}}_i|} + |\hat{\mathcal{N}}_i|\right)$.

V. Numerical Results

In this section, we evaluate the performance of the proposed method based on a real-world dataset. We use the offshore wind data at Roland island recorded by National Renewable Energy Laboratory (NREL) [22]. This dataset obtained from [22] is referred to as 5-min-wind, which contains the wind speed and direction with 5-min resolution. Dataset 5-min-wind can be regarded as the measurements collected by the remote sensing with UAVs. Traditionally, the resolution of the wind data for forecasting is 1 hr. Therefore, we construct the wind data with 1-hour resolution from 5-min-wind, referred to as

TABLE I
FORECASTING ACCURACY UNDER DIFFERENT DATASET

	Wind Speed		Wind Direction	
Method	MAE	RMSE	MAE	RMSE
Remote Sensing	0.0403	0.0573	0.0596	0.1151
Hour Ahead	0.0719	0.0972	0.1051	0.1687

1-hr-wind, for comparison. Then, forecasting the wind with 1-hr-wind is referred to as hour-ahead forecasting.

The make of the UAVs used in the simulation is AscTec Falcon 8. It is embedded with Lidar sensors to inspect turbines. It has a flight time between 12 and 22 minutes; so we set t_i^{max} to 18 minutes. The airspeed is limited to 16 m/s. The maximum resistance of the UAV to the wind speed is 15 m/s. The placement of UAVs in the wind farm and the turbines assigned to UAVs are solved by K-means clustering and non-linear integer programming [23].

The make of the turbine used in the simulation is SG 8.0-167 DD from Siemens. The swipe area, A, is 21900 square meter. The rated power is 8 MW and λ is set to $0°$. The tip speed ratio is generated according to the relation mentioned in [17]. The air density, ρ, is set to $1.065\text{kg}/\text{m}^3$.

For wind forecasting, we utilize the wind data from previous 2 hrs to forecast the wind data for next 40 mins. In the LSTM, it has a hidden layer with 100 nodes and is implemented in TensorFlow 1.13 with the Python 3.7.7. We compare the mean absolute error (MAE) and root mean square error (RMSE) as defined by (15) for performance comparison.

$$MAE = \sum_{i=1}^{n} \frac{|y_i - \hat{y}_i|}{n}, RMSE = \sqrt{\sum_{i=1}^{n} \frac{(y_i - \hat{y}_i)^2}{n}}. \quad (15)$$

In the simulation, MAE is used as the loss function of the LSTM network.

A. Wind Forecasting Result

For solving both optimization problems, we utilize LSTM for forecasting wind speed and direction. We first compare the performance of wind forecasting by utilizing remote sensing with traditional hour-ahead forecasting. Then, we introduce quantization to the LSTM. We compare the accuracy with and without quantization and find out how many bits are enough for wind forecasting.

The forecasting results with dataset 5-min-wind and 1-hr-wind are provided in Table I. According to the results, the MAE for forecasting the wind speed and the wind direction with hour-ahead forecasting is 0.0719 and 0.1051, respectively. However, the wind forecast with remote sensing yields 43% reduction on MAE compared to the hour-ahead forecasting. The improvement in terms of RMSE shows comparable numbers. This implies that remote sensing can considerably improve the accuracy of wind forecasting.

The accuracy of forecasting wind speed and wind direction under different quantization is shown in Table II. For the first row, ω_w and ω_f with both float32 (32-bit floating point) represent wind forecasting without quantization. Then, we compare the scenario where weights are quantized with 16-bit, 8-bit, 4-bit, and 2-bit fixed-point integer. According to the results, we can obtain similar accuracy as the forecasting without quantization if we further quantize the weight to 4 bits. In this case, we only require one-eighth storage space compared to the conventional LSTM using 32-bit floating point.

TABLE II
FORECASTING ACCURACY UNDER DIFFERENT BITS FOR QUANTIZATION

		Wind Speed		Wind Direction	
ω_w	ω_f	MAE	RMSE	MAE	RMSE
float32	float32	0.0403	0.0573	0.0596	0.1151
16	16	0.0396	0.0554	0.0609	0.1192
8	8	0.0392	0.0579	0.0608	0.1191
4	4	0.0401	0.0571	0.0598	0.1183
2	2	0.0431	0.0614	0.0807	0.1308

TABLE III
THE WIND POWER GENERATION UNDER DIFFERENT WIND DATA

Method	θ_w^{pol}(deg.)	Generation in an hour (kWh)	Generation in a day (kWh)
True	10	129	19861.2077
Remote Sensing	16	127	17952.1253
Hour Ahead	49	44	12428.0077

B. Power Generation with Yaw Control

We apply the results of wind forecasting as input to the yaw control to compare the power generation. In this section, we compare power generation of a wind turbine for an hour and for a day. We input the real wind data, the forecasting results using remote sensing, and forecasting results of using hour-ahead forecasting to Algorithm 1 and then compare the power generation in Table III. In Table III, we list the forecasted angle and then calculate the corresponding power generation for an hour. We can observe that we lose 2 kW of power generation in an hour if we forecast wind with remote sensing. However, a huge difference between forecasted and real wind direction occurs when utilizing hour-ahead forecasting. The incorrect wind direction can lead to non-optimal power generation from the turbines which means considerable loss in terms of huge loss on the power generation. We observe that with our proposed framework, we can obtain 44.45% increase in power generation in a day if we forecast the wind with remote sensing compared to hour-ahead forecasting.

C. Routing with Results of Wind Forecasting

Finally, we input the forecasted wind data to Algorithm 2 to solve the routing problem. We compare Algorithm 2 with the algorithms for finding the optimal routing paths in [21]. A diagram showing all UAVs and all turbines may lack clarity, and therefore we provide the results with two UAVs here. The location of the UAVs and the turbines assigned to them are presented in Fig. 3. In Fig. 3, UAV 1 and 2 are responsible for inspecting 5 and 2 turbines, respectively. Then, we consider a wind condition with $w_s = 10$ m/s and θ_w^{met} to $\frac{\pi}{2}$ (east wind). The routing results are summarized in Table IV.

In Table IV, we compare the routing results with and without using Algorithm 2. The total inspection time without using the proposed algorithm is 40.5051 mins. This is because UAV 1 faces head wind when flying to inspect turbine E105

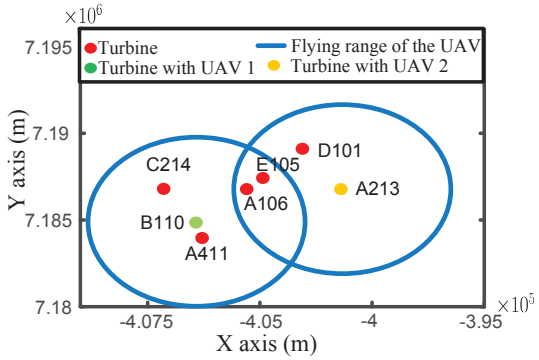

Fig. 3. The coordinates of UAVs and turbines.

TABLE IV
THE ROUTING RESULTS WITH AND WITHOUT DYNAMIC ASSIGNMENT

Method	t^{ins}(mins)	i	$path$
Algorithms in [21]	40.5051	1	B110>C214>>A106>B110
			B110>E105>A411>B110
		2	A213>D101>A213
Algorithm 2	30.0741	1	B110>C214>A106>A411>B110
		2	A213>D101>E105>A213

and A106. Thus, UAV 1 may leave these 2 turbines for the next round. Going back to the starting point and then starting another round for inspection takes extra time. By using Algorithm 2, E105 is outside the flying range of UAV 1. In this case, E105 is assigned to UAV 2 for inspection. If the Algorithm 2 is utilized, we can temporarily assign E105 to UAV 2 under this wind condition. By doing so, both UAVs only require one round to finish the inspection. Moreover, the total inspection time is reduced to 30.0741 mins, which is equivalent to 25% reduction in inspection time.

VI. Conclusion

In this paper, we presented a framework of utilizing UAVs as the computing units and remote sensing units for offshore wind farms. Then, we formulated two optimization problems to maximize the power generation of wind turbines and minimize the flight time for inspection. To solve the formulated problems, we used wind forecasting as the input. Conventional LSTM requires huge storage space and complex computation. We utilized quantization and sparse matrix computation to address the issue of the limited resources on the UAVs. With the forecasted result, we presented two algorithms to solve the optimization problems. We utilized real-world data to evaluate the proposed method. With the proposed framework, wind turbines can reach close to the maximum power generation and reduce the inspection time by 25%.

VII. Acknowledgements

This work was supported by Norwegian Research Council under Grants 275106 (LUCS project), 287412 (PACE project), and 267967 (SmartNEM project).

References

[1] European Commission, "Renewable Energy," https://ec.europa.eu/research/energy/index.cfm?pg=area&areaname=renewable_wind.
[2] J. Ribrant and L. M. Bertling, "Survey of Failures in Wind Power Systems With Focus on Swedish Wind Power Plants During 1997–2005," *IEEE Trans. Energy Convers.*, vol. 22, no. 1, pp. 167–173, Mar. 2007.
[3] K. Branner and A. Ghadirian, "Database about Blade Faults," DTU Wind Energy E-0067, Tech. Rep. 978-87-93278-09-7, Dec. 2014.
[4] L. Wang and Z. Zhang, "Automatic Detection of Wind Turbine Blade Surface Cracks Based on UAV-Taken Images," *IEEE Trans. Ind. Electron.*, vol. 64, no. 9, pp. 7293–7303, Sep. 2017.
[5] L. Wang, Z. Zhang, and X. Luo, "A Two-Stage Data-Driven Approach for Image-Based Wind Turbine Blade Crack Inspections," *IEEE/ASME Trans. Mechatronics*, vol. 24, no. 3, pp. 1271–1281, Jun. 2019.
[6] B. E. Schäfer, D. Picchi, T. Engelhardt, and D. Abel, "Multicopter Unmanned Aerial Vehicle for Automated Inspection of Wind Turbin," in *Proc. Medit. Conf. Control Autom. (MED)*, Athens, Greece, Jun. 2016, pp. 244–249.
[7] R. Yang, Y. He, A. Mandelis, N. Wang, X. Wu, and S. Huang, "Induction Infrared Thermography and Thermal-Wave-Radar Analysis for Imaging Inspection and Diagnosis of Blade Composites," *IEEE Trans. Ind. Informat.*, vol. 14, no. 12, pp. 5637–5647, Dec. 2018.
[8] J. R. Gallion and R. Zoughi, "Millimeter-Wave Imaging of Surface-Breaking Cracks in Steel With Severe Surface Corrosion," *IEEE Trans. Instrum. Meas.*, vol. 66, no. 10, pp. 2789–2791, Oct. 2017.
[9] M. Aghaei, F. Grimaccia, C. A. Gonano, and S. Leva, "Innovative Automated Control System for PV Fields Inspection and Remote Control," *IEEE Trans. Ind. Electron.*, vol. 62, no. 11, pp. 7287–7296, Nov. 2015.
[10] G. J. Lim, S. Kim, J. Cho, Y. Gong, and A. Khodaei, "Multi-UAV Pre-Positioning and Routing for Power Network Damage Assessment," *IEEE Trans. Smart Grid*, vol. 9, no. 4, pp. 3643–3651, Jul. 2018.
[11] J. R. T. Neto, A. Boukerche, R. S. Yokoyama, D. L. Guidoni, R. I. Meneguette, J. Ueyama, and L. A. Villas, "Performance Evaluation of Unmanned Aerial Vehicles in Automatic Power Meter Readings," in *Proc. Ad Hoc New.*, vol. 60, no. C, Amsterdam, The Netherlands, May 2017, pp. 11–25.
[12] S. Y. Derakhshandeh, Z. Mobini, M. Mohammadi, and M. Nikbakht, "UAV-Assisted Fault Location in Power Distribution Systems: An Optimization Approach," *IEEE Trans. Smart Grid*, vol. 10, no. 4, pp. 4628–4636, Jul. 2019.
[13] P. Cao, Y. Liu, C. Yang, S. Xie, and K. Xie, "MEC-Driven UAV-Enabled Routine Inspection Scheme in Wind Farm Under Wind Influence," *IEEE Access*, pp. 179 252–179 265, Dec. 2019.
[14] X. Lu, L. Xiao, C. Dai, and H. Dai, "UAV-Aided Cellular Communications with Deep Reinforcement Learning Against Jamming," *arXiv*, Apr. 2019. [Online]. Available: https://arxiv.org/abs/1805.06628
[15] G. Wu, Y. Miaoa, Y. Zhang, and A. Barnawi, "Energy Efficient for UAV-enabled Mobile Edge Computing Networks: Intelligent Task Prediction and Offloading," *IEEE Geosci. Remote Sens. Mag.*, vol. 150, no. 4, pp. 556–562, Jan. 2020.
[16] Y. Zhong, X. Wang, Y. Xu, S. Wang, T. Jia, X. Hu, J. Zhao, L. Wei, and L. Zhang, "Mini-UAV-Borne Hyperspectral Remote Sensing: From Observation and Processing to Applications," *IEEE Geosci. Remote Sens. Mag.*, vol. 6, no. 4, pp. 46–62, Dec. 2018.
[17] L.-R. Chang-Chien, C.-C. Sun, and Y.-J. Yeh, "Modeling of Wind Farm Participation in AGC," *IEEE Trans. Power Syst.*, vol. 29, no. 3, pp. 1204–1211, May 2014.
[18] M. Kuschke and K. Strunz, "Energy-Efficient Dynamic Drive Control for Wind Power Conversion With PMSG: Modeling and Application of Transfer Function Analysis," *IEEE Trans. Emerg. Sel. Topics Power Electron*, vol. 2, no. 1, pp. 35–46, Mar. 2014.
[19] Q. He, H. Wen, S. Zhou, Y. Wu, C. Yao, X. Zhou, and Y. Zou, "Effective Quantization Methods for Recurrent Neural Networks," *arXiv*, Nov. 2016. [Online]. Available: https://arxiv.org/abs/1611.10176
[20] S. Han, H. Mao, and W. J. Dally, "Deep Compression: Compressing Deep Neural Networks with Pruning, Trained Quantization and Huffman Coding," in *Proc. Intl. Conf. on Learn. Rep. (ICLR)*, Caribe Hilton, Puerto Rico, May 2016.
[21] P. Maini, K. Sundar, M. Singh, S. Rathinam, and P. B. Sujit, "Cooperative Aerial–Ground Vehicle Route Planning With Fuel Constraints for Coverage Applications," *IEEE Trans. Aerosp. Electron. Syst.*, vol. 55, no. 6, pp. 3016–3028, Dec. 2019.
[22] C. Draxl, A. Clifton, B.-M. Hodgea, and J. McCaa, "The Wind Integration National Dataset (WIND) Toolkit," *Appl. Energy*, vol. 151, pp. 355–366, Aug. 2015.
[23] J. Sun and C. Masouros, "Deployment Strategies of Multiple Aerial BSs for User Coverage and Power Efficiency Maximizationl," *IEEE Trans. Commun.*, vol. 67, no. 4, pp. 2981–2994, Apr. 2019.